

Article

Not peer-reviewed version

---

# Varying Synthesis Parameters on Potato Starch Aerogel for Aerospace Applications

---

Jacob Staker , [Daniel A Scheiman](#) , [Janice Mather](#) , [Jamesa L Stokes](#) , [Haiquan Guo](#) \*

Posted Date: 29 May 2025

doi: 10.20944/preprints202505.2334.v1

Keywords: potato starch; aerogel; biodegradable; thermal insulation; sustainability



Preprints.org is a free multidisciplinary platform providing preprint service that is dedicated to making early versions of research outputs permanently available and citable. Preprints posted at Preprints.org appear in Web of Science, Crossref, Google Scholar, Scilit, Europe PMC.

Copyright: This open access article is published under a Creative Commons CC BY 4.0 license, which permit the free download, distribution, and reuse, provided that the author and preprint are cited in any reuse.

Disclaimer/Publisher's Note: The statements, opinions, and data contained in all publications are solely those of the individual author(s) and contributor(s) and not of MDPI and/or the editor(s). MDPI and/or the editor(s) disclaim responsibility for any injury to people or property resulting from any ideas, methods, instructions, or products referred to in the content.

Article

# Varying Synthesis Parameters on Potato Starch Aerogel for Aerospace Applications

Jacob Staker <sup>1</sup>, Daniel A. Scheiman <sup>2</sup>, Janice Mather <sup>3</sup>, Jamesa L. Stokes <sup>4</sup> and Haiquan Guo <sup>2,\*</sup>

<sup>1</sup> Department of Chemistry, Purdue University

<sup>2</sup> Universities Space Research Association

<sup>3</sup> University of Akron

<sup>4</sup> NASA Glenn Research Center

\* Correspondence: haiquan.n.guo@nasa.gov

**Abstract:** Aerogels have many potential uses in common and higher tech aerospace application. Silica aerogels are fragile, and organic aerogels are tougher, but they are generally synthesized using toxic solvents. Biodegradable aerogels, if they possess similar properties as polymer aerogels, will widely be utilized in many aerospace applications and offer environmental benefits. In this work, potato starch aerogels were systematically studied. The potato starch concentration, the amount of plasticizer (glycerol), and an acid source (acetic acid) were varied. The relationship of the precursors on potato starch aerogel properties, such as density, shrinkage, porosity, BET surface area, mechanical properties, and thermal conductivities, were studied. The resulting potato starch aerogels possess suitable density, Young's modulus, and thermal conductivity for usability in many aerospace applications.

**Keywords:** potato starch; aerogel; biodegradable; thermal insulation; sustainability

## 1. Introduction

Aerogels are highly sought after energy efficient materials that can be used for many applications, especially as thermal insulation materials for aerospace due to their lightweight and low thermal conductivity [1]. Silica aerogels and silica-based aerogels are a widely used choice in this field because they are capable of retaining their mesoporous structure at high temperatures. However, they are mechanically brittle and fragile, limiting their feasibility for continuous use [2]. Many other aerogels have also been developed, including carbon aerogels [3], polyimide aerogels [4–10], polyamide aerogels [5], and polyurethane aerogels [6]. Since 2009, polyimide aerogels have opened up more opportunities for various aerospace applications, such as thermal insulation [7], nanogenerators [8], antenna substrates [9], and IR scattering filters [10]. However, to fabricate polyimide aerogels, toxic organic solvents like *n*-methylpyrrolidone (NMP), dimethylformamide (DMF), and dimethylacetamide (DMAc) are generally used [11]. The United States Environmental Protection Agency's (EPA) risk evaluation in 2020 found that NMP can cause serious health effects, including miscarriages and reduced fertility. Furthermore, NMP can cause harm to many organs and bodily systems, such as liver, kidneys, immune system, and the nervous system. Because of these risks, in June 2024, the EPA announced a proposed rule under the Toxic Substances Control Act (TSCA) and an NMP Workplace Chemical Protection Program (WCPP). If finalized, this will restrict the usage of NMP in the near future due to concerns for workers' health [12]. In addition to the syntheses involving organic toxic solvents, many polymers are difficult to decompose, thus also causing environmental harm [13]. Many organizations, like the EPA, across the globe are fighting to protect the environment. Environmentally friendly processes are currently on the rise in many commercial fields, including in the aerospace sector, which desire sustainable materials to reduce environmental impact and enhance the recyclability of components.

The synthesis of bio-based aerogels generally involves using non-toxic solvents, such as water and ethanol. The lack of toxic solvents and main composition of the material from natural biopolymers makes these materials a promising sustainable alternative to standard aerogel chemistries for aerospace applications. Starch, as one of the most abundant biomaterials, has been fabricated into aerogels and explored extensively [14–18]. Currently, most research has been focused on the retrogradation process [15], effect of amylose and amylopectin the final properties of the aerogels [16], and fabrication with different drying methods [17]. Starch aerogels have also been investigated for potential applications in thermal insulation, drug delivery, and packing materials [14,18,19]. In particular, potato starch has been the most studied among all the other starch aerogels.

The goal of this work is to evaluate and optimize the properties potato starch aerogels such as density, thermal conductivity, thermal stability, and mechanical properties required for potential aerospace applications. For this purpose, a design of experiments was used to study the synthesis parameters such as potato starch concentration, acetic acid amount, and glycerol amount on the properties of potato starch aerogel including density, surface area, thermal conductivity, and compressive modulus. Potato starch gels were fabricated by reacting a mixture of acetic acid, glycerol, and potato starch in water at 100 °C, followed by room temperature aging, -20 °C freezing, and ethanol washing. Potato starch aerogels were then produced by supercritical extraction of the wet gels with CO<sub>2</sub>. The resulting potato aerogels had densities of 0.11-0.30 g/cm<sup>3</sup>, compressive moduli of 2.7-37.8 MPa, and thermal conductivities of 37.5-45.2 mW/mK, which were comparable to reported polyimide aerogel properties [4–10].

## 2. Results and Discussion

**Figure 1a** shows an exemplary optical image of the potato starch precursor used in this study. As seen in the image, the potato starch precursor exhibited oval, irregular, and round shaped granules ranging from 5-55 μm in size. For the initial study, the potato starch aerogels were prepared by heating the mixture of potato starch, acetic acid, glycerol, and water at two different temperatures: 60°C and 100°C. Gels made from mixtures at 100°C were sturdier than those made at 60°C and had higher surface areas. The retrogradation and solvent processes were further studied for the gels that were made at 100°C. As seen in **Figure 1b**, when the gel was washed directly in ethanol after one day of aging at room temperature (RT), the surface/skin of the aerogel was wrinkled and deformed. When the gel was directly put into the freezer (-20°C), followed by ethanol washing without one day RT aging, icicles formed on the surface of the aerogel. Finally, the sample that was aged for one day, frozen for one day (at -20°C), and then washed five times with ethanol had the most uniform structure with no icicle formation.

Retrogradation during the sol-gel process is normal for starch, where a more ordered structure is formed due to relaxation of the biopolymers. The fast retrogradation rate happens at 0-4 °C [20]. From observed morphology of the synthesized gels, RT aging and freezing were both necessary for the retrogradation process to be completed. If the gel was directly soaked in ethanol, the retrogradation process was disrupted, resulting in a wrinkled and distorted sample shape. Also, if the sample was directly frozen without RT aging, icicles formed at the surface of the aerogel, because the ice forming rate was faster than the retrogradation rate. From the authors' previous study of preparing mixtures at 60°C, it was observed that freezing the sample for two days significantly reduced the aerogel shrinkage [21] due to the completion of the retrogradation process accompanied by ice growth, which expanded the gel structure. The expansion of the structure due to the ice formation happened during the second day of deep freezing. For this study, it was important to investigate the effect of potato starch concentration, the amounts of acetic acid, and glycerol on the properties of the aerogels while ignoring the ice expanding effect during the second day. Thus, all the samples in this paper were prepared at 100°C, aged at RT for one day, frozen at -20°C for one day, and then washed with ethanol five times.

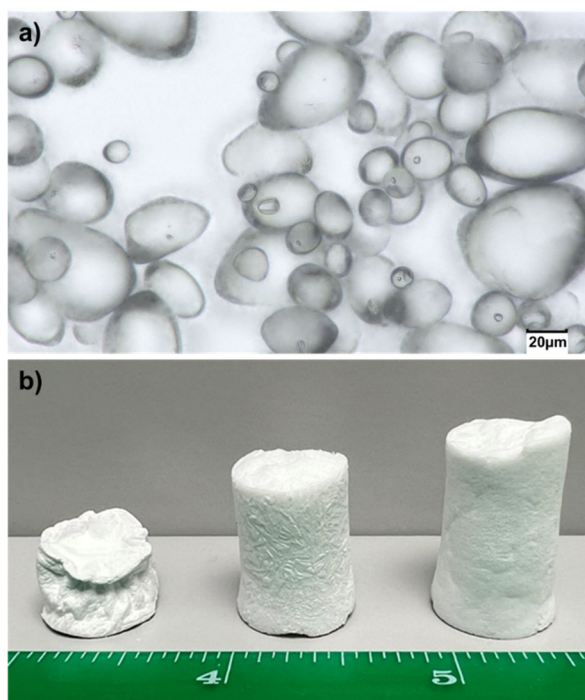


**Figure 1.** a) Optical microscope image of pure potato starch and b) potato starch aerogels that were prepared by (left) being directly soaked in ethanol after one day RT aging; (middle) one day frozen at  $-20^{\circ}\text{C}$  directly without one day RT aging, and then followed with ethanol wash; (right) one day RT aging, one day frozen at  $-20^{\circ}\text{C}$ , followed by ethanol wash.

The potato starch aerogels were prepared by varying the concentration of potato starch from 5wt%-10wt%, the potato starch to acetic acid ratios from 25 to 75, and glycerol to potato starch ratio from 0.5 to 0.75. The detailed formulations and the properties of resulting the potato starch aerogels are listed in **Table 1**.

**Table 1.** The formulation and properties of the potato starch aerogels.

Run	Potato Starch, wt%	Potato starch: Acetic acid	Glycerol: potato starch	Density, g/cm <sup>3</sup>	Shrinkage, %	Porosity, %	Surface area, m <sup>2</sup> /g	Young's modulus, MPa	Thermal conductivity, mW/mK
1	10	75	1	0.235	26.8	84.4	172.0	12.4	42.6
2	10	50	0.75	0.232	26.7	84.5	151.6	37.4	44.3
3	7.5	50	0.5	0.277	36.0	77.6	70.5	13.7	38.1
4	7.5	75	0.75	0.216	32.2	86.0	78.3	23.9	42.5
5	10	75	0.5	0.278	33.2	78.4	109.7	37.8	45.2
6	7.5	50	1	0.170	25.9	88.3	157.3	9.9	41.7
7	7.5	50	0.75	0.178	28.2	86.0	109.9	15.8	41.4
8	7.5	50	0.75	0.174	25.4	87.9	137.6	8.1	39.9
9	5	50	0.75	0.106	25.3	91.1	160.1	5.6	37.2
10	5	25	1	0.104	26.4	92.8	170.7	2.7	37.7
11	10	25	1	0.222	24.7	84.6	163.3	30.4	43.1
12	7.5	50	0.75	0.163	25.3	89.7	112.4	25.1	38.1
13	5	75	1	0.118	28.1	89.5	198.6	14.5	37.5

14	5	25	0.5	0.123	28.6	91.5	159.1	5.4	37.9
15	7.5	50	0.75	0.200	27.6	87.3	73.4	21.2	39.2
16	10	25	0.5	0.295	32.7	80.5	175.3	19.3	42.9
17	5	75	0.5	0.114	27.0	92.2	175.3	7.8	37.5
18	7.5	25	0.75	0.164	24.6	89.5	138.1	24.2	40.6

The densities of the potato starch aerogels ranged from 0.104 g/cm<sup>3</sup> to 0.295 g/cm<sup>3</sup>, the shrinkages ranged from 24.6% to 36%, and the porosities ranged from 77.6% to 92.8%. **Figure 2** shows empirical models for the relationships of density (standard deviation = 0.023 g/cm<sup>3</sup>, R<sup>2</sup>=0.90), shrinkage (standard deviation = 1.2%, R<sup>2</sup>=0.84), and porosity (standard deviation = 1.8%, R<sup>2</sup>=0.84) with potato starch weight percentage, potato starch to acetic acid ratio, and glycerol to potato starch ratio. Both the potato starch concentration and glycerol amount effected the density, shrinkage, and porosity of the aerogels. Acetic acid, which acted as a chain breakage agent, was found to have no effect on density, shrinkage, and porosity. With increasing potato starch concentration, the density increased significantly, the corresponding porosity decreased, and the shrinkage increased slightly at lower glycerol amounts but decreased at higher glycerol amounts. From the density plot, it shows that a 0.8 glycerol to potato starch ratio at 5 wt.% potato starch resulted in the lowest density aerogel. In the shrinkage plot, as the glycerol amount increased, the shrinkage of the aerogels decreased. At the lower potato starch concentration, the glycerol amount did not have a significant effect on the porosity. However, at higher potato starch concentrations, as the glycerol amount increased, the porosity increased. The amount of potato starch determined the mass of the aerogel monolith. Glycerol crosslinks the starch chains, which affects the final volume of the aerogel. The combination of these two, potato starch concentration and glycerol amount, affected the final density, shrinkage, and porosity, which in turn influenced the observed trends.

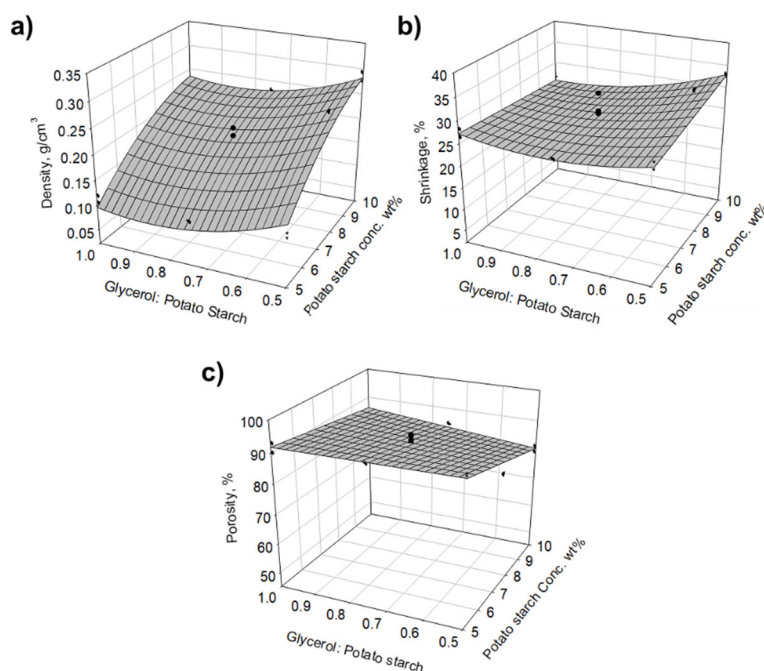


**Figure 2.** The empirical model plots of the relationship of a) density, b) shrinkage, and c) porosity.

N<sub>2</sub> adsorption / desorption was conducted to study the surface area and pore size distribution of the samples. **Figure 3a** shows the empirical model plots of the BET surface area of the aerogels (standard deviation = 16.65 m<sup>2</sup>/g, R<sup>2</sup>=0.84). The surface areas of the samples ranged from 70.3-198.6 m<sup>2</sup>/g. As the glycerol amount increased, the surface area increased. The potato starch concentration

also had an effect on the surface area. A concentration of 7.5 wt% potato starch resulted in the lowest surface area. **Figure 3b** shows the pore size-pore volume distribution plot of the potato starch aerogels. The pore volume and major pore size increased with potato starch concentration decreasing, which is similar to the porosity trend observed in **Figure 2c**. With acetic acid increasing, pore volume decreased. Increasing glycerol amount resulted in an increasing of pore volume and a larger major pore size. For example, the formulation with 10 wt% potato starch, potato starch: acetic acid ratio of 75, and a glycerol: potato starch ratio of 0.5 had a major pore size of 8.7 nm, and a BJH desorption cumulative pore volume 0.46 cm<sup>3</sup>/g, while a formulation with the same potato starch concentration and potato starch: acetic ratio with a glycerol: potato starch ratio of 1 had a major pore size of 15.6 nm, and a BJH desorption cumulative pore volume 0.84 cm<sup>3</sup>/g.

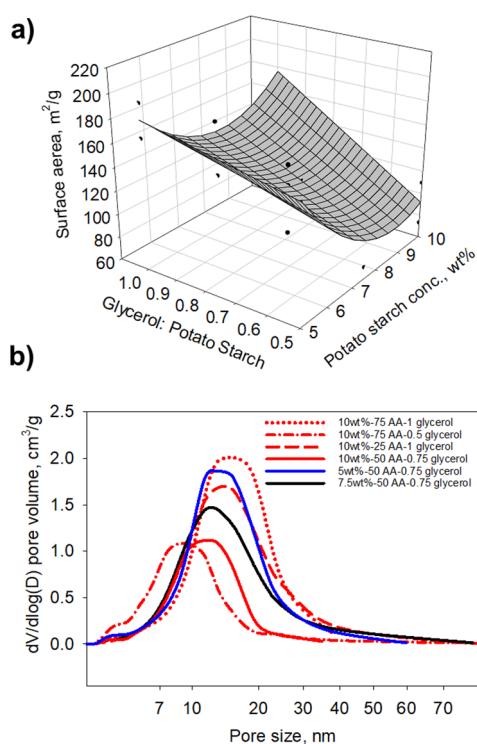


**Figure 3.** a) The empirical surface area of the potato starch aerogels. b) Pore size and pore volume distribution of the potato starch aerogels.

**Figure 4a** shows the typical thermogravimetric analysis (TGA) curves of the potato starch aerogels analyzed in nitrogen and in air. There was an initial solvent and moisture loss before 100°C. At 312°C, the potato aerogels exhibited immense mass loss, indicated decomposition occurring at this temperature. In air, there was a second decomposition step observed at 494°C, which was probably the onset of oxidation of the remaining char after 312°C. The potato starch aerogels had a char yield of about 20% in N<sub>2</sub> at 800°C. Thus, carbon aerogels were yielded by heating the potato starch aerogel at 800°C in argon gas, as seen in **Figure 4b**. Carbon aerogels can have a higher application temperature up to 2500°C in inert gas or vacuum environments [22], so they can be potentially used in aerospace, and energy storage applications where high temperature stability is required. Using potato aerogels to produce carbon aerogels is a more sustainable method than pyrolysis of other polymer aerogels. The carbon aerogel did not have a uniform diameter, but it contained a stable structure. It was observed that the carbon aerogels shape could be controlled by the crucible shape used, heating temperature, and heating and cooling rate, which might affect the outgassing during the pyrolysis process. As seen in the scanning electron microscope (SEM) images (**Figure 5**), the pore sizes of carbon aerogels in the macropore ranges increase, which was due to the release of CO<sub>2</sub>, CO, and H<sub>2</sub>O during the pyrolysis process. The surface area of the carbon aerogel decreased from 156.1

m<sup>2</sup>/g to 86.9 m<sup>2</sup>/g, which was due to the decrease of the pore volumes of 0-100 nm during the pyrolysis.

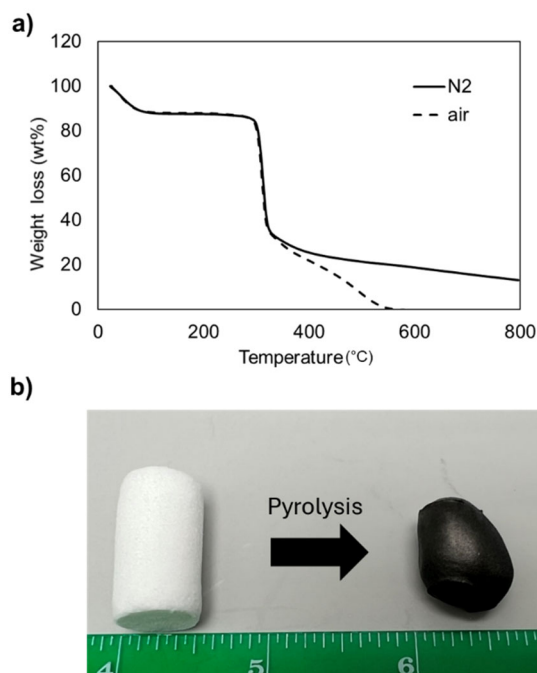


**Figure 4.** a) Typical TGA curves of potato starch aerogels analyzed in N<sub>2</sub> and air. b) Photo of a carbon aerogel (right) pyrolyzed from the potato starch formulation of 10 wt% potato starch, potato starch: acetic acid = 50, glycerol: potato starch = 0.75.

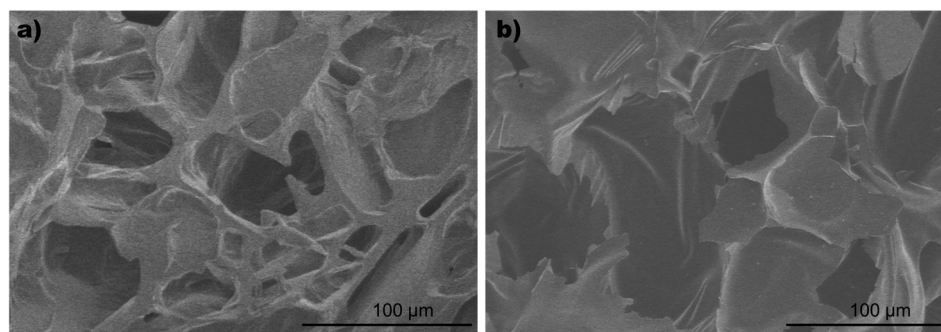


**Figure 5.** Scanning electron microscope images of a) potato starch aerogel with 10 wt% potato starch, potato starch: acetic acid = 50, glycerol: potato starch = 0.75; b) carbon aerogel pyrolyzed from aerogel (a).

Potato starch aerogel cylindrical monoliths were prepared for compression testing as shown in **Figure 6a**. At a constant displacement rate of 0.05 in./min, the aerogel was compressed until a measured force of 450 lbf. **Figure 6b** shows the selected stress-strain curves from the compression test of the potato starch aerogels. The Young's modulus was calculated from the initial slope of the elastic region of the aerogels. The Young's moduli of the aerogels ranged from 2.7 MPa to 37.8 MPa, which was higher than silica aerogels and comparable with some polyimide or polyamide aerogels [5]. As a result, potato starch aerogels will have potentially wider applications than silica aerogels and are more sustainable than polyimide aerogels. Seen from the empirical model plot (**Figure 6c**) of the Young's moduli ( $\log_{10}(\text{standard deviation}) = 0.18$ ,  $R^2 = 0.74$ ) of the potato starch aerogels, a higher the potato starch concentration resulted in a higher elastic modulus. Unlike density, the glycerol amount had no significant effect on the modulus. Instead, the acetic acid influenced the modulus, where increasing acetic acid resulted in slight modulus decrease. Acetic acid helps reducing the branch structure of amylopectin in the potato starch and shift to more linear amylose like structure,

which is attributed to the decreasing modulus. Although glycerol cross-links the potato starch chains, due to it is much shorter linkage compared to potato starch, the strengthening effect could not be observed by increasing the glycerol amount.

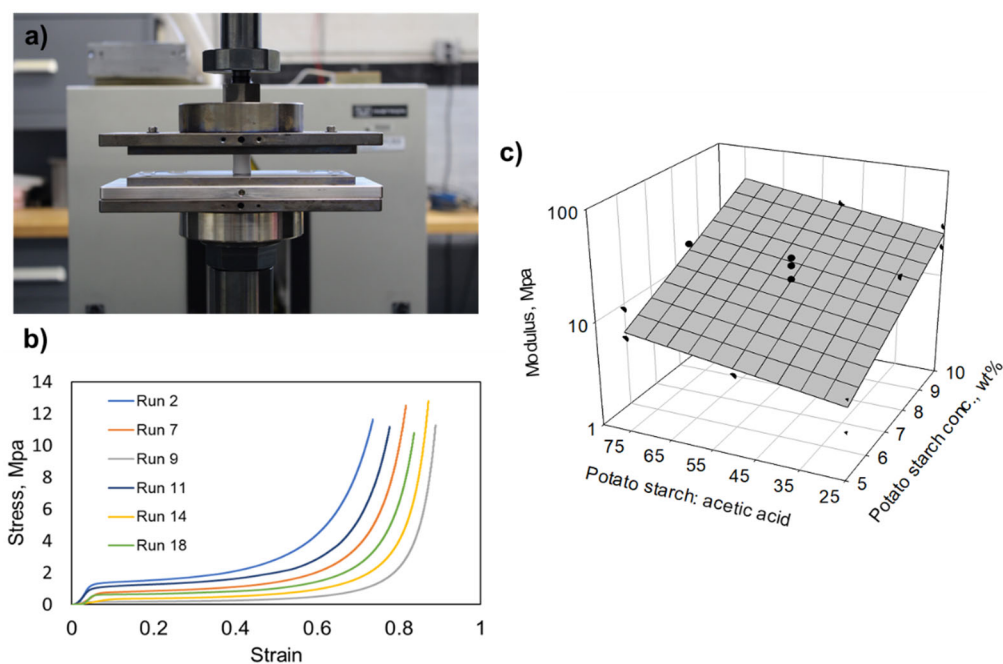


**Figure 6.** a) Image of a potato starch aerogel in the compression test setup; b) the stress-strain curves of potato starch aerogels; c) empirical model plot of compression Young's modulus of potato aerogels.

It was interesting to observe that potato starch aerogels can also be recycled. The potato starch aerogels can be grounded into powders that can be reused as the precursor. Following for the same sol-gel process, the powder was reformed into new potato starch aerogels. **Figure 7** shows the wet gels made from the recycled potato aerogel powders and the resulting new aerogels. Potato starch is an abundant resource on earth, and a biodegradable material. Recyclability of potato starch aerogels could also help reduce waste accumulation in the environment, making these materials even more sustainable for various applications.

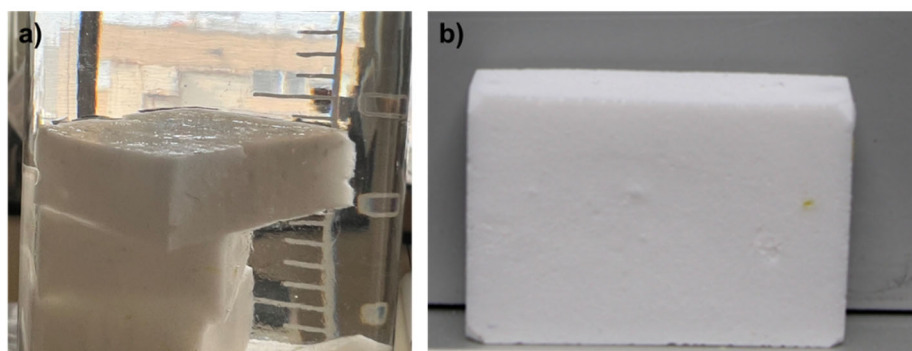


**Figure 7.** a) Wet gels made from recycled potato starch aerogel powders; b) potato aerogels made from the wet gels in a) to prove recyclability.

Because the potato starch aerogels have a large amount of hydroxyl groups on the surface of the aerogels, water can be absorbed very quickly. However, an aerogel that was floated on water was observed to remain floating after one week. At this time the aerogel was removed from the water so that total time the aerogel could float was speculated might be longer. The structure of the aerogel

remained intact with a little swell in size. Water was trapped inside the pores. In addition, no significant structural change was observed when it was exposed to moisture in the air after a year. Since the structure of potato starch aerogel can be retained in water, a simple solvent exchange in ethanol can remove the water and return to an aerogel again. For applications where aerogel need to be hydrophobic, the backbone of the potato starch aerogel can be modified with aliphatic groups to make it hydrophobic [23]. Future research can include modification of potato starch aerogels with aliphatic groups.

The measured thermal conductivities of the potato starch aerogels ranged from 37.5 mW/mK to 45.2 mW/mK. The empirical model plot of the thermal conductivity (standard deviation = 1.25,  $R^2=0.79$ ) of the potato starch aerogels was shown in **Figure 8**. The thermal conductivity greatly depended on the potato starch concentration, but not on the amounts of acetic acid or glycerol. Higher the potato concentrations resulted in higher thermal conductivities. The thermal conductivity of the potato starch aerogels was also higher than silica aerogels [24] but was close to some reported polyimide aerogels [25,26], and lower than many insulation materials [27] currently in use.

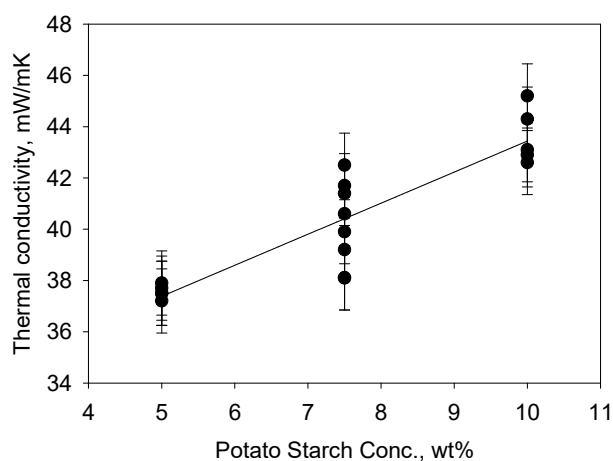


**Figure 8.** The empirical model plot of the thermal conductivity of the potato starch aerogels.

### 3. Conclusions

Potato starch aerogels were made with 5-10 wt% potato starch; potato starch: acetic acid ratios ranged from 25-75, and glycerol: potato starch ratios varied from 0.5 to 1. The aerogels made by utilizing the higher temperature process were sturdier and had higher surface areas. It was found both room temperature aging and deep-frozen processes were necessary to make well-structured aerogels. Potato starch concentration has a great impact on all the properties investigated. Acetic acid had no effect on density, shrinkage, porosity, surface area, but affected pore volumes and mechanical properties. The glycerol amount slightly affected density, shrinkage, porosity, pore sizes and surface area, but not Young's modulus. Thermal conductivity only depended on potato starch concentration. The resulting potato starch aerogels were not only biodegradable, recyclable, and economical, but also their density (0.11-0.30 g/cm<sup>3</sup>), mechanical modulus (2.7-37.8 MPa), and thermal conductivity (37.5-45.2 mW/mK) were all applicable for thermal insulation materials, comparable to polyimide aerogels. Although the potato starch aerogels absorb water easily, they retain their structure while holding water, and can always be washed with ethanol and remade into aerogels. Potato starch aerogels can also be pyrolyzed into carbon aerogels for higher temperature aerospace applications. In summary, the green synthesis route, the biodegradability and recyclability of the material, and desired properties of the potato starch aerogels in our design make them potential sustainable materials for aerospace applications.

### 4. Materials and Methods

#### 4.1. Materials Used for Aerogel Formulations

GEFEN pure potato starch was used in the research. 99.7% acetic acid and glycerol were obtained from Sigma Aldrich. Distilled water was prepared from lab.

#### 4.2. Method for Fabricating Aerogel Including Supercritical Drying

The formulations of the potato starch aerogels were listed in Table 1. The potato starch concentration was varied from 5-10 wt%. The ratio of potato starch to acetic acid ratio ranged from 25 to 75. The ratio of glycerol to potato starch ranged from 0.5 to 1. For example, run 1 was prepared as following: a mixture of 5g potato starch, 5g glycerol, 0.063ml acetic acid, and 49.333 ml H<sub>2</sub>O was heated by an oil bath until it boiled and formed a viscous sol. The viscous sol was poured in a cylinder mold. The sol was aged at RT for 1day, and then put in freezer at -20°C for 1day, and the gels were extracted into ethanol and washed with ethanol daily for five times. The resulted gel was dried by supercritical extraction with CO<sub>2</sub>.

#### 4.3. Experimental Design and Analysis

Design Expert, version 13 from Stat-Ease, Inc. (Minneapolis, MN, USA) was used to conduct experimental design and analysis. Three variables (potato starch concentration, (5-10 wt%), potato starch:acetic acid ratio (25-75), and acetic acid:glycerol ratio (0.5-1)) were used in the experimental design. A total of 18 aerogel formulations with four repeats with central composite design were prepared as shown in Table 1. Multiple linear regression was used to analyze the collected data. A full quadratic equation of the variables, including all two-way interactions, was considered for each response, and terms deemed not significant were eliminated from the model.

#### 4.4. Bulk Density, Shrinkage and Porosity Determination

The bulk density  $\rho$  (g/cm<sup>3</sup>) of each aerogel sample is calculated by mass and its volume,

$$\rho = \frac{m}{v_c}, \quad (1)$$

where  $m$  is sample mass (g), and  $v_c = \pi d^2 h/4$  is the volume (cm<sup>3</sup>), where  $d$  and  $h$  are the sample's diameter and length, respectively.

The sample linear shrinkage  $S$  (%) is determined by the relative change diameter,

$$S (\%) = 100 \times \frac{d_0 - d_x}{d_0}, \quad (2)$$

where  $d_0$  is the initial gel diameter, also the mold diameter.  $d_x$  is the diameter of aerogel monoliths.

A Micromeritics Accupyc li 1345 (Norcross, GA, USA) helium pycnometer was utilized to measure skeleton density ( $\rho_s$ ) of the samples in a 10 cm<sup>3</sup> micromeritics cell with cap. The aerogel porosity  $P_t$  (%) was calculated as following.

$$P_t (\%) = 100 \times \left(1 - \frac{\rho}{\rho_s}\right) \quad (3)$$

#### 4.5. Instrument Characterization

Aerogel samples were degassed at 80 °C overnight. Nitrogen adsorption-desorption was conducted using a Micromeritics Tristar 3020 II (Norcross, GA, USA) to determine the surface areas, pore sizes, and absorption/desorption curves of the aerogel samples. Scanning electron microscopy (SEM) was used to obtain micrographs of the aerogels using a Hitachi S-4700 field emission microscope. Trident C-Therm (Fredericton, New Brunswick, CAN), conforming to ASTM D7984, was used to conduct the measurement of the thermal conductivities of the aerogels. Thermogravimetric analysis (TGA) was performed with TA Instruments Q500 TGA (New Castle, DE, USA) with a heat ramp rate of 10°C/min. Compressive testing was performed using an Instron electromechanical load frame (model 5584) with Bluehill control software. An Interface load cell with a full calibrated range of 500 lbf with a corresponding error of 1% of reading, or better, was used. The aerogel sample was

compressed at a constant displacement rate of 0.05 in./min until 450 lbf was measured. Force and displacement data was collected at a frequency of 500 Hz during the compression.

**Author Contributions:** The manuscript was written through contributions of all authors. All authors have given approval to the final version of the manuscript. Jacob Staker performed all the experiments, collected the data, and edited the paper. Daniel Scheiman conducted TGA, pycnometry test, and edited the paper. Janice Mather conducted compression test and edited the paper. Dr. Jamesa L. Stokes supervised the work, performed SEM, and edited the paper. Dr. Haiquan Guo supervised and designed the experiment, conducted nitrogen adsorption-desorption test, measured thermal conductivity, analyzed all the data, and edited the paper. All authors have read and agreed to the published version of the manuscript.

**Funding:** This research was funded by the Indiana Space Grant Consortium (INSGC).

**Institutional Review Board Statement:** Not applicable.

**Informed Consent Statement:** Not applicable.

**Data Availability Statement:** Not applicable.

**Acknowledgments:** We thank NASA Glenn Research Office of STEM Engagement (OSTEM) and the Indiana Space Grant Consortium. We also wish to thank Dr. Amanda P. Siegel and Dr. Andres Tovar from Indiana University-Purdue University Indianapolis for their support with potato starch.

**Conflicts of Interest:** The authors declare no conflicts of interest.

## References

1. Bheekhun, N. ; Talib, A. R. A. ; Hassan, M. R. Aerogels in aerospace: An overview. *Adv. Mater. Sci. Eng.* **2013**, *2013*, 406065.
2. Dorchen, A. S.; Abbasi, M. H. Silica aerogel; synthesis, properties and characterization. *J. Mater. Proc. Tech.* **2008**, *199*, 10-26.
3. Baptista, J. M.; Sagu, J. S.; KG, U. W.; Lobato, K. State-of-the-art materials for high power and high energy supercapacitors: Performance metrics and obstacles for the transition from lab to industrial scale – A critical approach. **2019**, *374*, 1153-1179.
4. Guo, H.; Meador, M. A. B.; McCorkle, L.; Quade, D. J.; Guo, J.; Hamilton, B.; Cakmak, M.; Sprow, G. Polyimide Aerogels Cross-Linked through Amine Functionalized Polyoligomeric Silsesquioxane. *ACS Appl. Mater. Interfaces* **2011**, *3*, 546–552.
5. Scheiman, D. A.; Guo, H.; Oosterbaan, K. J.; McCorkle, L.; Nguyen, B.N. Synthesis of Polyamide Aerogels Cross-Linked with a Tri-isocyanate. *Gels* **2024**, *10*, 519.
6. Merillas, B.; León, J. M.; Villafañe, F.; Rodríguez-Pérez, M. A. Transparent Polyisocyanurate-Polyurethane-Based Aerogels: Key Aspects on the Synthesis and Their Porous Structures. *ACS Appl. Polym. Mater.* **2021**, *3*, 4607–4615.
7. Bruce III, W. E.; Mesick, N. J.; Ferlemann, P. G.; Siemers III, P. M.; Del Corso, J. A.; Hughes, S. J.; Tobin, S. A.; Kardell, M. Aerothermal Ground Testing of Flexible Thermal Protection Systems for Hypersonic Inflatable Aerodynamic Decelerators. 9<sup>th</sup> International Planetary Probe Workshop, Toulouse, France, 16-22 JUNE 2012.
8. Mi, H.-Y.; Jing, X.; Meador, M. A. B.; Guo, H.; Turng, L.-S.; Gong, S. Triboelectric Nanogenerators Made of Porous Polyamide Nanofiber Mats and Polyimide Aerogel Film: Output Optimization and Performance in Circuits. *ACS Appl. Mater. Interfaces* **2018**, *10*, 30596-30606.
9. Guo, H.; Meador, M.A. B.; Cashman, J. L.; Tresp, D.; Dosa, B.; Scheiman, D. A.; McCorkle, L. S. Flexible Polyimide Aerogels with Dodecane Links in the Backbone Structure. *ACS Appl. Mater. Interfaces* **2020**, *12*, 33288-33296.
10. Barlis, A.; Guo, H.; Helson, K.; Bennett, C.; Chan, C. Y. Y.; Marriage, T.; Quijada, M.; Tokarz, A.; Vivod, S.; Wollack, E.; Essinger-Hileman, T. Fabrication and characterization of optical filters from polymeric aerogels loaded with diamond scattering particles. *Applied Optics* **2024**, *63*, 6036-6045.
11. Xu, Z.; Croft, Z.; Guo, D.; Cao, K.; Li, G. Recent development of polyimides: Synthesis, processing, and application in gas separation. *J. Poly. Sci.* **2021**, *59*, 943-962.

12. n-Methylpyrrolidone (NMP); Revision to Toxic Substances Control Act (TSCA) Risk Determination; Notice of Availability. Environmental Protection Agency. 87 FR 77596, 2022-27438, 12/19/2022, 77596-77602.
13. Wang, Y., Airborne hydrophilic microplastics in cloud water at high altitudes and their role in cloud formation. *Environmental Chemistry Letters* **2023**, *21*, 3055-3062.
14. Kumar, K.; Saxena D. C.; A Review on Starch Aerogel: Application and Future Trends. 8th International Conference on Advancements in Engineering and Technology, (ICAET-2020) BGIET, Sangrur, ISBN No: 978-81-924893-5-3.
15. Huang, S.; Chao, C.; Yu, J. Coperland, L.; Wang, S. New insight into starch retrogradation: The effect of short-range molecular order in gelatinized starch. *Food Hydrocolloids* **2021**, *120*, 106921.
16. Jiamjariyatam, R.; Kongpensook, V.; Pradipasena, P.; Effects of amylose content, cooling rate and aging time on properties and characteristics of rice starch gels and puffed products. *J. of Cereal Sci.* **2014**, *61*, 16–25
17. Zou, F.; Budtova, T.; Tailoring the morphology and properties of starch aerogels and cryogels via starch source and process parameter. *Carbohydrate Polymers* **2021**, *255*, 117344.
18. Druel, L.; Bardl, R.; Vorwerg, W.; Budtova, T. Starch aerogels: A member of the family of thermal superinsulating materials. *Biomacromolecules* **2017**, *18*, 4232– 4239.
19. Franco, P.; De Marco, I. Supercritical CO<sub>2</sub> adsorption of non-steroidal anti-inflammatory drugs into biopolymer aerogels. *J. CO<sub>2</sub> Utilization* **2020**, *36*, 40-53.
20. Aguirre, J. F.; Osella, C. A.; Carrara, C. R.; Sa´ nchez, H. D.; Buera, M. del P. Effect of storage temperature on starch retrogradation of bread staling. *Starch/Sta`rke* **2011**, *63*, 587–593.
21. Staker, J.; White, G. M.; Pasilova, S.; Scheiman, D. A.; Guo, H.; Tovar, A.; Siegel, A. P. Mitigating Shrinkage and Enhancing Structure of Thermally Insulating Starch Aerogel via Solvent Exchange and Chitin Addition. *Macromol* submitted.
22. Hu, L.; He, R.; Lei, H.; Fang, D. Carbon Aerogel for Insulation Applications: A Review. *International Journal of Thermophysics* **2019**, *40*, 39
23. Namazi, H.; Fathi, F.; Dadkhah A. Hydrophobically modified starch using long-chain fatty acids for preparation of nanosized starch particles. *Scientia Iranica* **2011**, *18*, 439-445.
24. Fu, Z.; Corker, J.; Papathanasiou, T.; Wang, Y.; Zhou, Y.; Madyan, O. M.; Liao, F.; Fan, M. Critical review on the thermal conductivity modelling of silica aerogel composites. *J. of Building Engineering* **2022**, *57*, 104814-104840.
25. Feng, J.; Wang, X.; Jiang, Y.; Du, D.; Feng, J. Study on Thermal Conductivities of Aromatic Polyimide Aerogels. *ACS Appl. Mater. Interfaces* **2016**, *8*, 12992–12996.
26. Yang, J.; Lu, J.; Xi, S.; Wang H.; Han, D.; Fan, C.; Zhang, Z.; Shen, J.; Zhou, B.; Du, A. Direct 3D print polyimide aerogels for synergy management of thermal insulation, gas permeability and light absorption. *J. Mater. Chem. A* **2023**, *11*, 21272-21284.
27. Zhang, S., Waang, Z.; Wang, J.; Xiao, Y.; Yang, Z., Ji, H.; Xu, G.; Xiong, S.; Li, Z.; Ding F. Polyimide Aerogels with Excellent Thermal Insulation, Hydrophobicity, Machinability, and Strength Evolution at Extreme Conditions. *ACS Appl. Polym. Mater.* **2022**, *4*, 8227–8237.

**Disclaimer/Publisher’s Note:** The statements, opinions and data contained in all publications are solely those of the individual author(s) and contributor(s) and not of MDPI and/or the editor(s). MDPI and/or the editor(s) disclaim responsibility for any injury to people or property resulting from any ideas, methods, instructions or products referred to in the content.